Biomedical Optics EXPRESS

Characterization of internodal collecting lymphatic vessel function after surgical removal of an axillary lymph node in mice

Sunkuk Kwon[1,*] and Roger E. Price[2]

[1]*Center for Molecular Imaging, The Brown Foundation Institute of Molecular Medicine The University of Texas Health Science Center, Houston, TX 77030, USA*
[2]*Comparative Pathology Laboratory, Center for Comparative Medicine, Baylor College of Medicine, Houston, Texas 77030, USA*
[*]*sunkuk.kwon@uth.tmc.edu*

Abstract: Secondary lymphedema is an acquired lymphatic disorder, which occurs because of damage to the lymphatic system from surgery and/or radiation therapy for cancer treatment. However, it remains unknown how post-nodal collecting lymphatic vessels (CLVs) draining to the surgical wound area change in response to lymphadenectomy. We investigated functional and architectural changes of inguinal-to-axillary internodal CLVs (ICLVs) in mice after a single axillary LN (ALN) dissection using near-infrared fluorescence imaging. Our data showed no lymph flow in the ICLVs draining from the inguinal LN (ILN) at 2 days post-surgery. External compression enabled visualization of a small segment of contractile fluorescent ICLVs, but not all the way to the axillary region. At day 6, abnormal lymphatic drainage patterns, including lateral and retrograde lymph flow via vessels branching off the ICLVs were observed, which started to disappear beginning 9 days after surgery. The administration of vascular endothelial growth factor (VEGF)-C into the wound increased resolution of altered lymphatic drainage. Lymphatic drainage from the base of the tail to the ILN did not significantly change over time. These results demonstrate that lymph flow in the CLVs is dramatically affected by a LN dissection and long-term interruption of lymph flow might cause CLV dysfunction and thus contribute to chronic lymphatic disorders.

OCIS codes: (170.0170) Medical optics and biotechnology; (170.0110) Imaging systems; (170.2655) Functional monitoring and imaging; (170.3880) Medical and biological imaging; (170.4580) Optical diagnostics for medicine.

References and links

1. Y. Wang and G. Oliver, "Current views on the function of the lymphatic vasculature in health and disease," Genes Dev. **24**(19), 2115–2126 (2010).
2. K. Alitalo, "The lymphatic vasculature in disease," Nat. Med. **17**(11), 1371–1380 (2011).
3. K. S. Blum, S. T. Proulx, P. Luciani, J. C. Leroux, and M. Detmar, "Dynamics of lymphatic regeneration and flow patterns after lymph node dissection," Breast Cancer Res. Treat. **139**(1), 81–86 (2013).
4. J. C. Zampell, A. Yan, S. Elhadad, T. Avraham, E. Weitman, and B. J. Mehrara, "CD4(+) cells regulate fibrosis and lymphangiogenesis in response to lymphatic fluid stasis," PLoS One **7**(11), e49940 (2012).
5. J. C. Zampell, A. Yan, T. Avraham, V. Andrade, S. Malliaris, S. Aschen, S. G. Rockson, and B. J. Mehrara, "Temporal and spatial patterns of endogenous danger signal expression after wound healing and in response to lymphedema," Am. J. Physiol. Cell Physiol. **300**(5), C1107–C1121 (2011).
6. U. Mendez, E. M. Brown, E. L. Ongstad, J. R. Slis, and J. Goldman, "Functional recovery of fluid drainage precedes lymphangiogenesis in acute murine foreleg lymphedema," Am. J. Physiol. Heart Circ. Physiol. **302**(11), H2250–H2256 (2012).
7. T. Tammela, A. Saaristo, T. Holopainen, J. Lyytikkä, A. Kotronen, M. Pitkonen, U. Abo-Ramadan, S. Ylä-Herttuala, T. V. Petrova, and K. Alitalo, "Therapeutic differentiation and maturation of lymphatic vessels after lymph node dissection and transplantation," Nat. Med. **13**(12), 1458–1466 (2007).

#255572 Received 14 Dec 2015; revised 8 Feb 2016; accepted 26 Feb 2016; published 3 Mar 2016

8. U. Mendez, E. M. Stroup, L. L. Lynch, A. B. Waller, and J. Goldman, "A chronic and latent lymphatic insufficiency follows recovery from acute lymphedema in the rat foreleg," Am. J. Physiol. Heart Circ. Physiol. **303**(9), H1107–H1113 (2012).
9. S. Kwon, G. D. Agollah, G. Wu, and E. M. Sevick-Muraca, "Spatio-temporal changes of lymphatic contractility and drainage patterns following lymphadenectomy in mice," PLoS One **9**(8), e106034 (2014).
10. E. M. Sevick-Muraca, S. Kwon, and J. C. Rasmussen, "Emerging lymphatic imaging technologies for mouse and man," J. Clin. Invest. **124**(3), 905–914 (2014).
11. S. Kwon and E. M. Sevick-Muraca, "Mouse phenotyping with near-infrared fluorescence lymphatic imaging," Biomed. Opt. Express **2**(6), 1403–1411 (2011).
12. S. Kwon and E. M. Sevick-Muraca, "Functional lymphatic imaging in tumor-bearing mice," J. Immunol. Methods **360**(1-2), 167–172 (2010).
13. S. Kwon and E. M. Sevick-Muraca, "Noninvasive quantitative imaging of lymph function in mice," Lymphat. Res. Biol. **5**(4), 219–232 (2007).
14. P. E. Lapinski, S. Kwon, B. A. Lubeck, J. E. Wilkinson, R. S. Srinivasan, E. Sevick-Muraca, and P. D. King, "RASA1 maintains the lymphatic vasculature in a quiescent functional state in mice," J. Clin. Invest. **122**(2), 733–747 (2012).
15. P. E. Burrows, M. L. Gonzalez-Garay, J. C. Rasmussen, M. B. Aldrich, R. Guilliod, E. A. Maus, C. E. Fife, S. Kwon, P. E. Lapinski, P. D. King, and E. M. Sevick-Muraca, "Lymphatic abnormalities are associated with RASA1 gene mutations in mouse and man," Proc. Natl. Acad. Sci. U.S.A. **110**(21), 8621–8626 (2013).
16. G. D. Agollah, M. L. Gonzalez-Garay, J. C. Rasmussen, I. C. Tan, M. B. Aldrich, C. Darne, C. E. Fife, R. Guilliod, E. A. Maus, P. D. King, and E. M. Sevick-Muraca, "Evidence for SH2 domain-containing 5′-inositol phosphatase-2 (SHIP2) contributing to a lymphatic dysfunction," PLoS One **9**(11), e112548 (2014).
17. S. Kwon, C. Davies-Venn, and E. M. Sevick-Muraca, "In vivo dynamic imaging of intestinal motions using diet-related autofluorescence," Neurogastroenterol. Motil. **24**(5), 494–497 (2012).
18. S. S. Bass, C. E. Cox, C. J. Salud, G. H. Lyman, C. McCann, E. Dupont, C. Berman, and D. S. Reintgen, "The effects of postinjection massage on the sensitivity of lymphatic mapping in breast cancer," J. Am. Coll. Surg. **192**(1), 9–16 (2001).
19. M. Mihara, H. Hara, Y. Hayashi, M. Narushima, T. Yamamoto, T. Todokoro, T. Iida, N. Sawamoto, J. Araki, K. Kikuchi, N. Murai, T. Okitsu, I. Kisu, and I. Koshima, "Pathological steps of cancer-related lymphedema: histological changes in the collecting lymphatic vessels after lymphadenectomy," PLoS One **7**(7), e41126 (2012).
20. E. Bazigou and T. Makinen, "Flow control in our vessels: vascular valves make sure there is no way back," Cell. Mol. Life Sci. **70**(6), 1055–1066 (2013).
21. K. Hayashi, P. Jiang, K. Yamauchi, N. Yamamoto, H. Tsuchiya, K. Tomita, A. R. Moossa, M. Bouvet, and R. M. Hoffman, "Real-time imaging of tumor-cell shedding and trafficking in lymphatic channels," Cancer Res. **67**(17), 8223–8228 (2007).
22. T. Kodama, Y. Hatakeyama, S. Kato, and S. Mori, "Visualization of fluid drainage pathways in lymphatic vessels and lymph nodes using a mouse model to test a lymphatic drug delivery system," Biomed. Opt. Express **6**(1), 124–134 (2015).
23. T. Karnezis, R. Shayan, C. Caesar, S. Roufail, N. C. Harris, K. Ardipradja, Y. F. Zhang, S. P. Williams, R. H. Farnsworth, M. G. Chai, T. W. Rupasinghe, D. L. Tull, M. E. Baldwin, E. K. Sloan, S. B. Fox, M. G. Achen, and S. A. Stacker, "VEGF-D promotes tumor metastasis by regulating prostaglandins produced by the collecting lymphatic endothelium," Cancer Cell **21**(2), 181–195 (2012).
24. M. A. Hall, H. Robinson, W. Chan, and E. M. Sevick-Muraca, "Detection of lymphangiogenesis by near-infrared fluorescence imaging and responses to VEGF-C during healing in a mouse full-dermis thickness wound model," Wound Repair Regen. **21**(4), 604–615 (2013).
25. Y. S. Yoon, T. Murayama, E. Gravereaux, T. Tkebuchava, M. Silver, C. Curry, A. Wecker, R. Kirchmair, C. S. Hu, M. Kearney, A. Ashare, D. G. Jackson, H. Kubo, J. M. Isner, and D. W. Losordo, "VEGF-C gene therapy augments postnatal lymphangiogenesis and ameliorates secondary lymphedema," J. Clin. Invest. **111**(5), 717–725 (2003).
26. A. Saaristo, T. Veikkola, T. Tammela, B. Enholm, M. J. Karkkainen, K. Pajusola, H. Bueler, S. Ylä-Herttuala, and K. Alitalo, "Lymphangiogenic gene therapy with minimal blood vascular side effects," J. Exp. Med. **196**(6), 719–730 (2002).
27. A. Szuba, M. Skobe, M. J. Karkkainen, W. S. Shin, D. P. Beynet, N. B. Rockson, N. Dakhil, S. Spilman, M. L. Goris, H. W. Strauss, T. Quertermous, K. Alitalo, and S. G. Rockson, "Therapeutic lymphangiogenesis with human recombinant VEGF-C," FASEB J. **16**(14), 1985–1987 (2002).
28. A. Aspelund, T. Tammela, S. Antila, H. Nurmi, V. M. Leppänen, G. Zarkada, L. Stanczuk, M. Francois, T. Mäkinen, P. Saharinen, I. Immonen, and K. Alitalo, "The Schlemm's canal is a VEGF-C/VEGFR-3-responsive lymphatic-like vessel," J. Clin. Invest. **124**(9), 3975–3986 (2014).
29. M. Hofmann, R. Pflanzer, N. N. Zoller, A. Bernd, R. Kaufmann, D. Thaci, J. Bereiter-Hahn, S. Hirohata, and S. Kippenberger, "Vascular endothelial growth factor C-induced lymphangiogenesis decreases tumor interstitial fluid pressure and tumor," Transl. Oncol. **6**(4), 398–404 (2013).
30. D. T. Sweet, J. M. Jiménez, J. Chang, P. R. Hess, P. Mericko-Ishizuka, J. Fu, L. Xia, P. F. Davies, and M. L. Kahn, "Lymph flow regulates collecting lymphatic vessel maturation in vivo," J. Clin. Invest. **125**(8), 2995–3007 (2015).
31. R. E. Mebius, P. R. Streeter, J. Brevé, A. M. Duijvestijn, and G. Kraal, "The influence of afferent lymphatic vessel interruption on vascular addressin expression," J. Cell Biol. **115**(1), 85–95 (1991).

#255572 Received 14 Dec 2015; revised 8 Feb 2016; accepted 26 Feb 2016; published 3 Mar 2016

32. H. Hoshi, K. Kamiya, H. Aijima, K. Yoshida, and E. Endo, "Histological observations on rat popliteal lymph nodes after blockage of their afferent lymphatics," Arch. Histol. Jpn. **48**(2), 135–148 (1985).
33. J. H. Wolfe, D. Rutt, and J. B. Kinmonth, "Lymphatic obstruction and lymph node changes--a study of the rabbit popliteal node," Lymphology **16**(1), 19–26 (1983).
34. G. Steinmann, E. Földi, M. Földi, P. Rácz, and K. Lennert, "Morphologic findings in lymph nodes after occlusion of their efferent lymphatic vessels and veins," Lab. Invest. **47**(1), 43–50 (1982).

1. Introduction

The lymphatic system plays an important role in tissue fluid homeostasis and immune surveillance [1]. The lymphatic system consists of three main components; (i) initial, pre-collecting, and collecting lymphatic vessels, (ii) lymphoid tissues such as lymph nodes (LNs), spleen, and thymus, and (iii) lymph. It has been shown that abnormal function in each component is implicated in a number of pathological conditions including edema, obesity, and autoimmune diseases [2]. For example, when lymphatic vessels do not function normally due to inherent disorder of or damage to the lymphatics from surgery, radiation therapy, trauma or infection, the abnormal buildup of fluid in tissues occurs. Yet despite the importance of the lymphatics in disease, diagnostic imaging approaches to non-invasively monitor lymphatic vessel function lag behind. More importantly, it is still largely unknown how lymphatic drainage differs in different body regions and responds to an insult such as surgery. Unlike whole body blood vascular imaging, which is readily preformed following intravenous (i.v.) injection of contrast agents, only a few lymphatic vessels which drain the injection area after intradermal (i.d.) injection of contrast agents are visualized. The lymphatic system allows only one-way transit of lymph from initial to gradually larger collecting lymphatic vessels and finally into the blood circulation.

Several animal models of secondary lymphedema have been previously developed by surgical removal of LNs and associated tissues such as an axillary LN dissection (ALND) model. In these models, lymphatic vessel function has been investigated using different imaging techniques [3–8]. In the ALND model, lymphatic drainage patterns were examined in response to surgical removal of the ALN alone or together with the brachial LN (BLN) [3–8]. Lymph from the front paw drains to the superficial BLN and then to the ALN. After axillary and/or brachial lymphadenectomy, transient changes of lymphatic drainage in the front paw were observed over time [3, 6–8]. For example, interstitial diffuse patterns from the operated limb were detected in early response to lymphadenectomy; however, extravascular drainage and dermal backflow disappeared eventually and lymphatic vessels bypassing the wound area were observed [6]. The ALN also receives lymph from the inguinal LN (ILN) through the internodal collecting lymphatic vessels. However, no studies have shown how post-nodal collecting lymphatic vessels draining to the surgical wound area change functionally and architecturally in response to axillary lymphadenectomy. In this study, we used dual-wavelength fluorescence imaging with injection of two different lymphatic mapping agents, Alexa-680-bovine serum albumin (BSA) and ICG, both of which have been used for lymphatic imaging [9, 10]. Unlike other imaging modalities, such as magnetic resonance imaging (MRI) and positron emission tomography (PET), fluorescence optical imaging allows simultaneous visualization of lymphatic vessels in different regions due to a distinct spectral wavelength emitted from each injected fluorophore.

The aim of the present study was to longitudinally image lymphatic vessels in the paw and the intermodal collecting lymphatic vessels in the trunk in mice after surgical removal of an ALN using dual-wavelength fluorescence imaging and to investigate how lymphatic function and drainage patterns change over time in response to surgery.

2. Materials and methods

2.1. Experimental animal models

Animals were maintained in a pathogen-free mouse facility accredited by the American Association for Laboratory Animal Care. All experiments were performed in accordance with the guidelines of the Institutional Animal Care and Use Committee. Animal experiments were

#255572 Received 14 Dec 2015; revised 8 Feb 2016; accepted 26 Feb 2016; published 3 Mar 2016

approved by University of Texas Health Science Center Institutional Animal Care and Usage Committee.

Eight to ten week old female C57BL/6 mice (n = 40; Charles River) were housed and fed sterilized pelleted food and sterilized water. Residual hair was removed with depilatory cream (Nair, Church & Dwight Co., Inc.) 24 hrs before surgery. Mice were anesthetized with isofluorane (2% oxygen) and maintained on a warming pad at 37 °C. A left ALN was detected after i.d. injection of 2 μl of 1% Evans blue dye (EBD) solution (5mg/ml; Sigma) into the dorsal aspect of the left paw. Bupivacaine (0.25%; 1 mg/kg) was given subcutaneously at the incision site and a small (~5 mm) incision was made with scissors through the skin. Subsequently, a blue ALN was carefully removed under a stereomicroscope (MZ16 A, Leica Microsystems, Inc.) through a minimally invasive approach, with minimal disruption to the surrounding tissues. Following ALN removal, wounds were closed with surgical glue (3M Vetbond). Buprenorphine (0.1 mg/kg) was administered intraperitoneally once after surgery. The day the surgery was performed was designated as day 0. Mice used in this study did not show infection and/or inflammation at the wound site at any imaging time point. The wrist diameter and arm area were measured using a stereomicroscope and the operated side was normalized to the contralateral right side.

2.2. Fluorescence lymphatic imaging

Animals were clipped and residual hair removed with depilatory cream 24 hrs before imaging. Mice anesthetized with isofluorane were maintained on a warming pad. At 24 hrs after clipping/nairing, mice were imaged at baseline prior to axillary lymphadenectomy and every 2 to 4 days for up to 37 days after surgery. A volume of 10 to 30 μl of 645 μM of indocyanine green (ICG; Akorn, Inc.) dissolved in a mixture of distilled water and 0.9% Sodium Chloride in a volume ratio of 1:9 was injected intradermally to the left side of base of the tail with 31 gauge needles (BD Ultra-fine II Insulin syringe). Fluorescence images were acquired immediately after and for up to 10 min after i.d. injection using a custom-built NIRFI system [11–15]. Dynamic NIRFI following i.d. injection of ICG was also performed in mice prior to surgery and then immediately after surgical removal of the ALN. After NIRFI, far-red fluorescence imaging (FRFI) was conducted 5 mins after i.d. injection of 2 μl of Alexa680- BSA to the dorsum of the left front paw. Mice were imaged longitudinally up to 37 days after surgery. External compression was made using a cotton swab pressed on the left ILN for 1 min after initial injection of ICG 2 days after lymphadenectomy (n = 4). In order to investigate the systemic effect of local lymphadenectomy, mice (n = 3) were also imaged on the right side prior to and up to 6 days after left axillary lymphadenectomy following i.d. injection of ICG to the right side of base of the tail. The sham-operated control mice underwent an incision of the left axillary area without an ALN dissection (n = 5).

In separate groups of mice, mice were daily treated for 9 days, starting one day before axillary lymphadenectomy by i.d. injection into the wound with 200 ng of human recombinant VEGF-C (Cys156Ser; R&D Systems) dissolved in 10 μl PBS (n = 11). The control group (n = 5) was injected with PBS alone.

2.3. Analysis of lymphatic vessel function

Matlab (The MathWorks, Inc., Natick, MA) and ImageJ (National Institutes of Health, Washington, DC) were used to analyze the fluorescence imaging data [9, 14]. To reveal lymphatic contractility, fixed regions of interest (ROIs) in fluorescent internodal collecting lymphatic vessels were defined on sequential frames of fluorescence images. The mean of the fluorescence intensity within each ROI in each fluorescence image was calculated and then plotted as a function of imaging time to assess the frequency of contraction along the lymphatic vessels. Thus, the frequency of contractile waves of ICG-laden lymph propelled along the lymphatic vessels was measured by assessing the number of fluorescent pulses or "packets" arriving at a ROI [14]. In addition, images were analyzed to assess lymphatic uptake at the injection site and the presence of abnormal lymphatic architecture such as dense

#255572 Received 14 Dec 2015; revised 8 Feb 2016; accepted 26 Feb 2016; published 3 Mar 2016

networks of lymphatic capillaries with extravascular fluorescence frequently known as dermal backflow [16].

2.4. Histology

Mice were sacrificed after 13 to 37 days. LNs as well as skin tissues containing internodal collecting lymphatic vessels were collected, weighed, fixed in 10% formalin, and submitted to the Center for Comparative Medicine, Comparative Pathology Laboratory, Baylor College of Medicine for routine histological processing, sectioning, hematoxylin and eosin (H&E) staining, and examination.

2.5. Statistical analysis

Data were presented as average values ± standard error (SE). Statistical analysis was performed with Prism 5 (Graphpad Software, Inc). All data were tested for normality using the D'Agostino–Pearson normality test prior to analysis. Changes of ankle diameter and leg area were analyzed with one-way repeated-measures analysis of variance (ANOVA) with a Bonferroni posttest for multiple comparisons over time. For the pairwise comparisons, the Wilcoxon matched pairs test was used. The Mann-Whitney test was also used when comparisons were made between two groups. The significance level is set as $p < 0.05$.

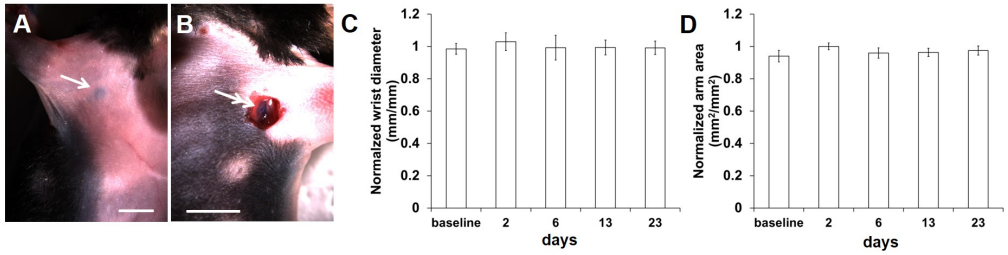

Fig. 1. Representative stereoscopic color images 5 mins after i.d. injection of EBD to the paw showing (A) the superficial left BLN filled with blue dye and (B) the deep ALN after skin incision. Arrow, BLN. Double arrow, ALN. Scale, 5 mm. Wrist thickness (C) and arm area (D) in mice (n = 6) were measured and the operated side was normalized to the contralateral right side.

3. Results

3.1. Lymphatic drainage is transiently altered after surgical removal of the ALN

EBD injection on the paw in mice delineated the superficial BLN as shown in Fig. 1(A). Subsequently, the left ALN was observed following a small incision in the skin over the axillary region (Fig. 1(B)). Axillary lymphadenectomy with minimal disruption to the surrounding tissues showed mild, non statistically significant, swelling of the operated front paw after surgery as measured by wrist diameter and arm area (Figs. 1(C) and 1(D)), showing that minimally invasive ALN dissection was not able to produce acute or chronic lymphedema.

#255572 Received 14 Dec 2015; revised 8 Feb 2016; accepted 26 Feb 2016; published 3 Mar 2016

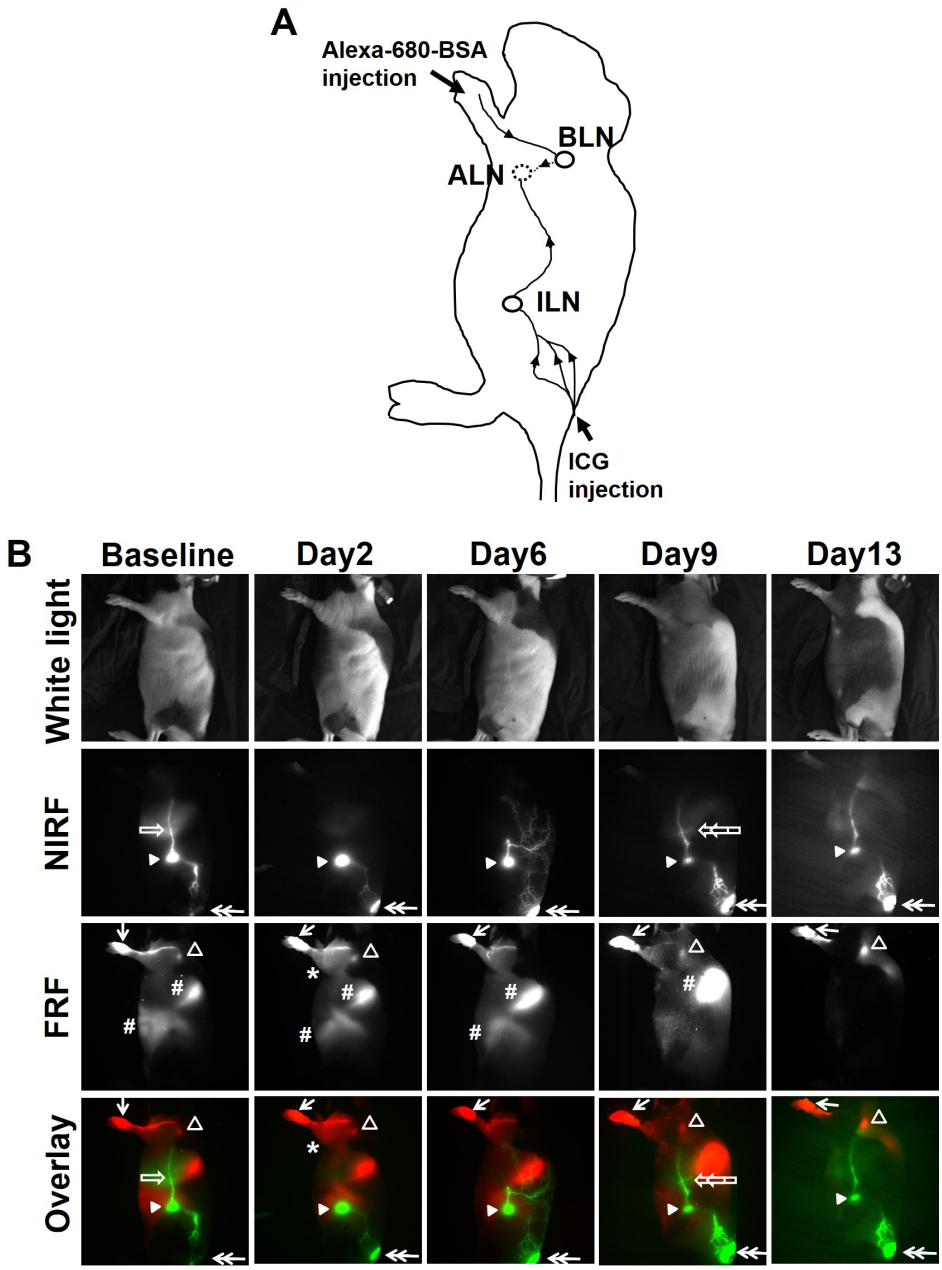

Fig. 2. A. Schematic of lymphatic drainage pathways from the base of the tail to the ILN and to the ALN after injection of ICG as well as from the paw to the BLN and to the ALN after injection of Alexa-680-BSA. The deeply located ALN and vessels are dotted. Arrow heads indicate flow direction. B. White light, NIR and FR fluorescent, and overlay images in mice prior to and 2, 6, 9, and 13 days after surgical removal of the left ALN. NIRF and FRF images were acquired 10 mins and 3 mins after i.d. injection of ICG or Alexa680-BSA, respectively. Double arrow, ICG injection site. Arrow, Alexa680-BSA injection site. Closed arrow head, ILN. Open arrow head, BLN, Open arrow, internodal collecting lymphatic vessels. Asterisk, abnormal lymphatic drainage patterns on the paw. Pound sign, FRF from the gut (see Visualization 1 and Visualization 2).

#255572 Received 14 Dec 2015; revised 8 Feb 2016; accepted 26 Feb 2016; published 3 Mar 2016

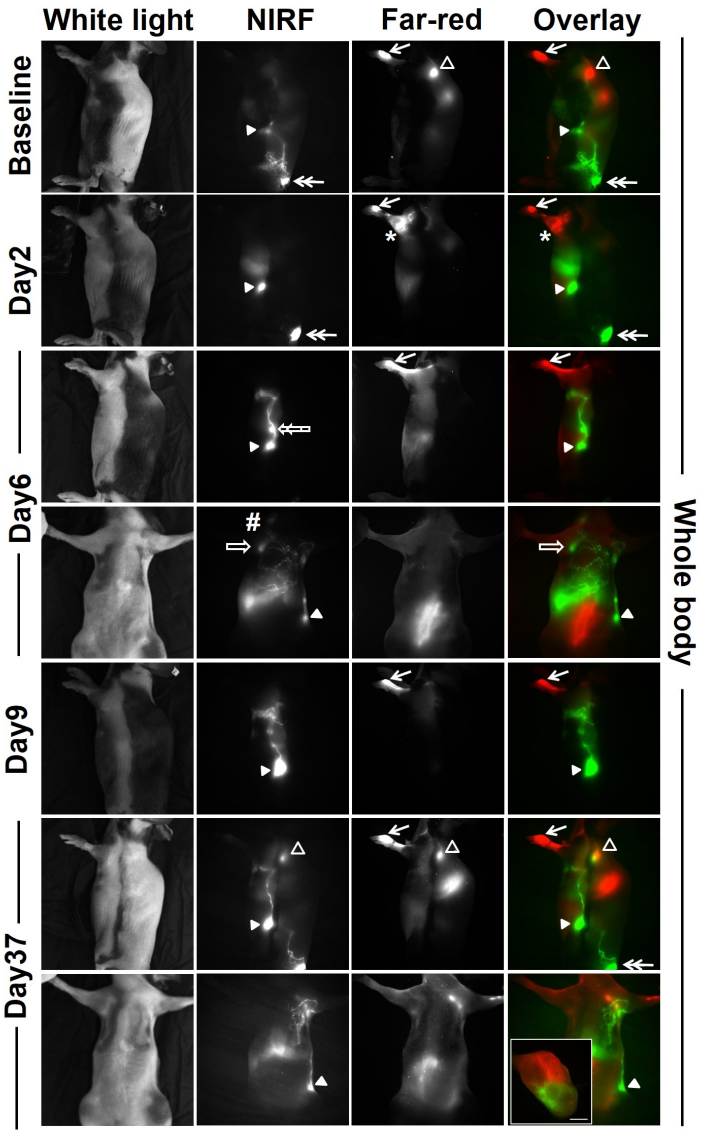

Fig. 3. White light, NIR and FR fluorescent, and overlay images in mice prior to and 2, 6, and 37 days after surgical removal of the left ALN. NIRF and FRF images were acquired 10 mins and 3 mins after i.d. injection of ICG or Alexa680, respectively. Double arrow, backflow. Arrow, Alexa680-BSA injection site. Closed arrow head, ILN. Open arrow head, BLN, Open arrow, right ALN. Asterisk, abnormal lymphatic drainage patterns on the paw. Inset at Day 37, overlay of NIR and FR fluorescent images of an excised BLN in the bottom row at Day 37. Scale, 1mm, (see Visualization 3).

All mice showed well-defined lymphatic vessels draining from the injection site on the base of the tail to the ILN and further drainage to the ALN through the internodal collecting lymphatic vessels prior to lymphadenectomy at baseline imaging following i.d. injection of ICG (Fig. 2). We also occasionally observed lymphatic vessels draining from the injection site to the internodal collecting lymphatic vessels (Fig. 5(A)). FRFI (Fig. 2) showed lymphatic drainage from the left front paw to the BLN before surgery at baseline. FRFI also showed fluorescence (pound sign in Fig. 2) generated from standard murine diet in the gastrointestinal tract [17]. The specific drainage pattern in each mouse was consistently observed in two baseline imaging sessions.

#255572 Received 14 Dec 2015; revised 8 Feb 2016; accepted 26 Feb 2016; published 3 Mar 2016

Previous studies showed abnormal lymphatic drainage in the front paw after surgical removal of the ALN and/or BLN; however, it is unknown how internodal collecting lymphatic vessels draining from the ILN to the ALN change in response to axillary lymphadenectomy. Longitudinal fluorescence lymphatic imaging demonstrated dramatic changes of lymphatic drainage patterns after axillary lymphadenectomy. At 2 days post-surgery, similar drainage patterns of afferent inguinal lymphatic vessels draining from the base of the tail to the ILN were observed in all mice. However, fluorescent collecting lymphatic vessels connecting from the left ILN to the ALN were not observed during dynamic imaging. An additional injection of 20 µl of ICG (a total of 30 µl) did not change lymphatic drainage patterns (data not shown). FRFI showed dermal backflow through dermal capillaries on the left paw at Day 2 (asterisk in Fig. 2). At 6 days post-surgery, we detected aberrant lymphatic drainage through the internodal collecting lymphatic vessels from the ILN. As shown in Fig. 2 and Visualization 1, lymph flow from the ILN was inhibited before reaching the axillary region and ICG-laden lymph drained laterally and backwards to the injection site, and eventually spread over the truncal region. In addition, there was an absence of pulsatile activity in lymphatic vessels that branched off from the internodal collecting lymphatic vessels (Visualization 1). At Day 6, we still observed abnormal drainage from the paw, although it was a less extensive lymphatic drainage pattern as compared to Day 2. Surprisingly, at Day 9, abnormal patterns on the trunk disappeared and fluorescent collecting lymphatic vessels connecting the ILN to the axillary region were observed, although only a few lymphatic vessels branching off the collecting lymphatic vessels were detected (double open arrow in Fig. 2). The same pattern of baseline lymphatic drainage on the paw was detected on day 9 post-surgery. From day 13, we could not detect altered lymphatic drainage patterns on the paw and trunk. Interestingly, lateral lymph flow toward the back of a mouse is detected through a segment of branched vessel, which shows pulsatile activity (Visualization 2).

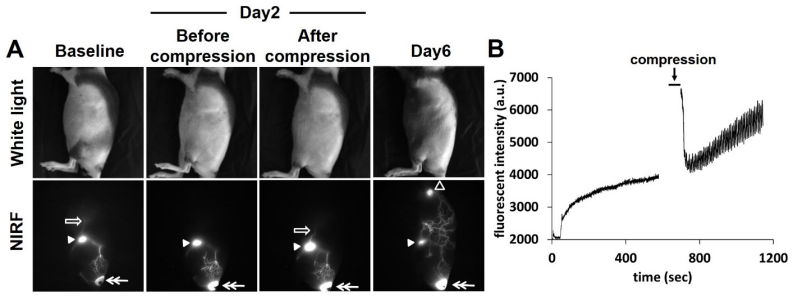

Fig. 4. A. White light and NIR fluorescent images in mice prior to and 2 and 6 days after axillary lymphadenectomy. At 2 days post-surgery, NIR fluorescent images were acquired before and after external compression to the ILN (n = 4). Double arrow, ICG injection site. Closed arrow head, ILN. Open arrow head, BLN, Open arrow, internodal collecting lymphatic vessels. B. The fluorescent intensity profiles as a function of time in mice after selecting a ROI in the collecting lymphatic vessels before and after compression for one min, (see Visualization 4).

Fluorescent lymphatic vessels draining to the contralateral ALN across the midline were also observed in mice that underwent left axillary lymphadenectomy. As shown in Fig. 3, NIRFI could not detect fluorescent collecting lymphatic vessels draining from the ILN to the ALN at 2 days post-surgery. Although pigmented skin around the paw attenuates fluorescent signal, lymphatic drainage from the paw to the BLN was detected from baseline FRFI. FRFI showed dermal backflow and extravascular Alex680-BSA on the operated limb at day 2. At 6 days after surgery, NIRFI demonstrated backflow of ICG-laden lymph, as evidenced by a bright spot (double open arrow in Fig. 3), and NIR fluorescent lymphatic vessels bypassing the wound area leading to the ipsilateral BLN and spreading laterally to the contralateral ALN (open arrow) and backwards to the abdominal region (Visualization 3). Interestingly, ICG laden lymph further drained to the right cervical LN (CLN; pound sign in Fig. 3).

#255572 Received 14 Dec 2015; revised 8 Feb 2016; accepted 26 Feb 2016; published 3 Mar 2016

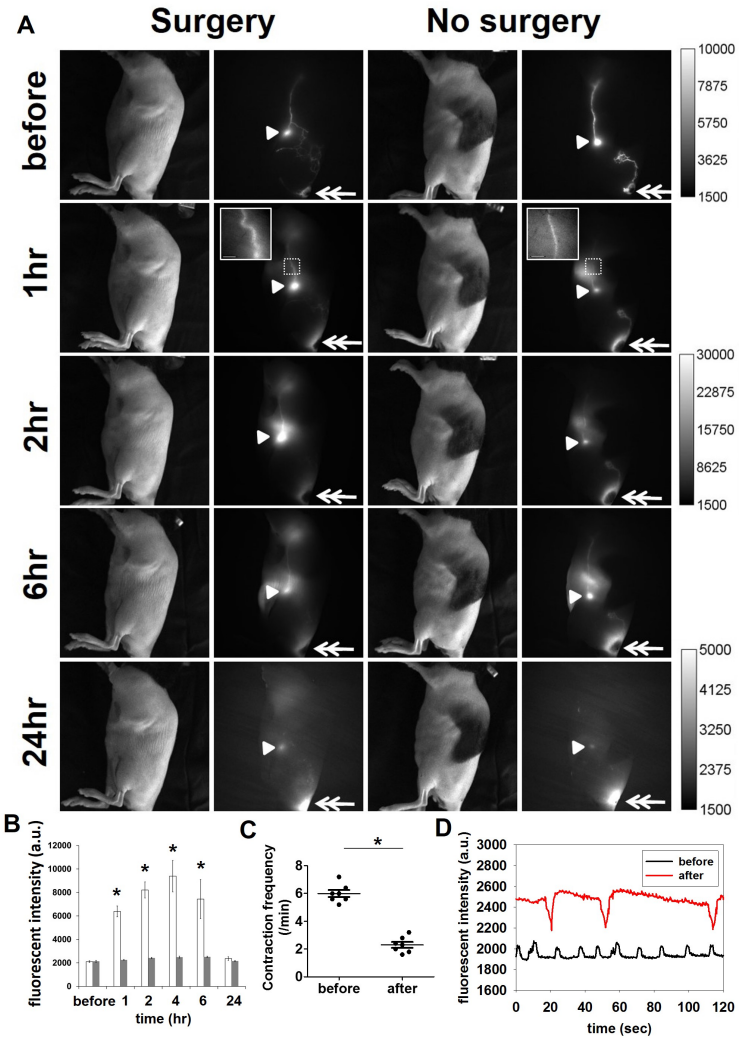

Fig. 5. A. White light and fluorescent images in the left lateral side of mice prior to and 1, 2, 6, and 24 hrs after ALN removal, following i.d. injection of ICG to the base of the tail. Double arrow, ICG injection site. Arrow head, ILN. Inset, magnified image of the white rectangle region. Scale, 1 mm. B. The fluorescent intensities in the axillary region in mice (white) before and up to 24 hrs after axillary lymphadenectomy and mice with no surgery (grey). * $p < 0.05$ vs. non-surgery mice (n = 7/group). C. The lymphatic contraction frequency in the internodal collecting lymphatic vessels before and 10 mins after surgery. D. Representative image demonstrating lymphatic vessel contraction (before, black; after, red). * $p < 0.05$.

We also observed these lymphatic drainage patterns at 9 days post-surgery, although abnormal patterns on the operated limb disappeared. At day 37, fewer NIR fluorescent lymphatic vessels proximal to the axillary region were observed and no ICG extravasation was observed. In addition, lymphatic drainage to the right ALN was not detected. Since the left BLN received lymph from both the left paw and the left ILN, we dissected and imaged the left BLN. Our dual-fluorescence imaging data (Fig. 3) demonstrated that the upper half of the BLN showed FRF due to the injection of Alexa680-BSA to the paw, whereas the lower half showed NIRF owing to the ICG trafficking.

We observed no changes in lymphatic drainage pathways in sham-operated controls 2 and 6 days after a skin incision.

#255572 Received 14 Dec 2015; revised 8 Feb 2016; accepted 26 Feb 2016; published 3 Mar 2016

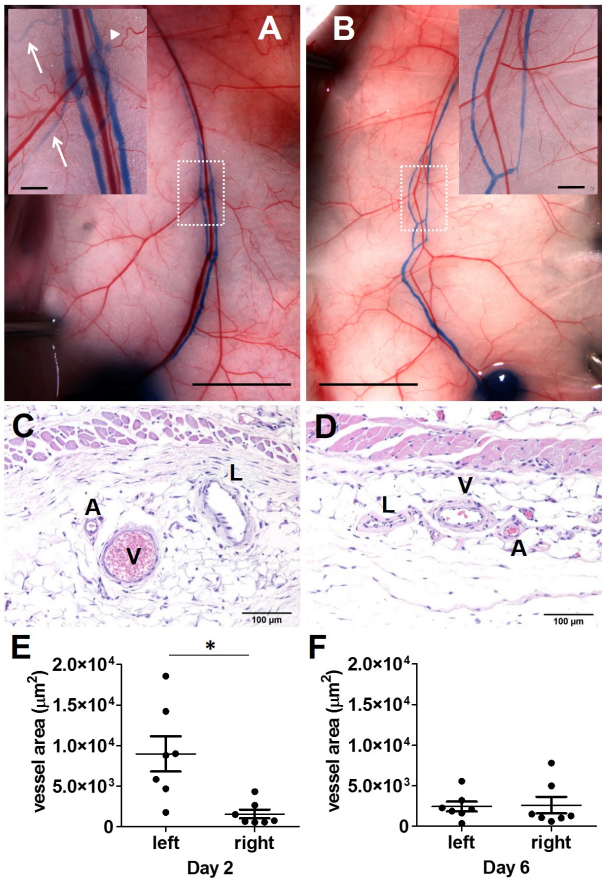

Fig. 6. Intravital color images after direct injection of EBD into the ILN (A, B) and H&E images (C, D) in mice with (A) or without axillary lymphadenectomy (B). Scale, 5 mm. Inset, magnified image of the white dotted rectangle region. Arrow, branching off lymphatic vessels. Arrow head, backflow of EBD. Scale, 500 μm. Quantification of collecting lymphatic vessel area (n = 7/group) at Day 2 (E) and Day 6 (F). * $p < 0.05$.

3.2. Effects of external compression on lymphatic drainage

At 2 days after axillary lymphadenectomy, mice showed no fluorescent internodal collecting lymphatic vessels during dynamic imaging, indicative of no lymph flow. Since external pressure can enhance lymph flow [18], we next applied external compression by pressing on the left ILN using a cotton swab for 1 min at 10 mins after initial injection of ICG at 2 days post-surgery. Before compression of the left ILN of mice, no lymphatic drainage from the ILN to the ALN as shown in Figs. 2 and 3 was detected (Fig. 4). However, after external compression, we observed a small segment of fluorescent internodal collecting lymphatic vessels draining from the ILN, but not all the way to the axillary region (open arrow; Visualization 4). The NIR fluorescent intensity profiles as a function of time from dynamic NIRFI (Visualization 4) also showed active lymph pumping activities in the segment of collecting lymphatic vessels (Fig. 4(B)). At day 6 post-surgery, we detected significant drainage over the truncal region without external compression.

#255572 Received 14 Dec 2015; revised 8 Feb 2016; accepted 26 Feb 2016; published 3 Mar 2016

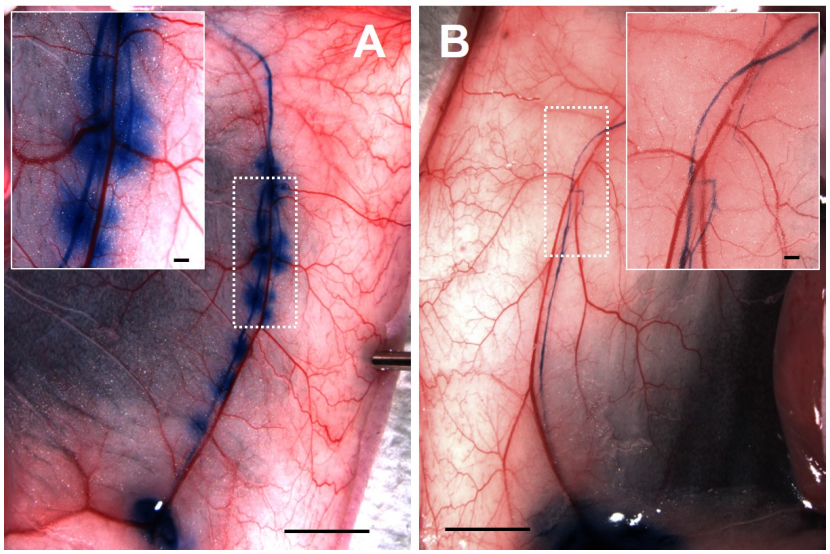

Fig. 7. Representative stereoscopic color images immediately after i.d. injection of EBD into the ILN, showing backflow of EBD-laden lymph in mice at 2 days post-surgery (A) as compared to control mice (B). Scale, 5 mm. Inset, magnified image of the white dotted rectangle region. Scale, 100 μm.

3.3. Effects of lymph node removal on collecting lymphatic vessels

Lymph draining from the ILN to the ALN is ultimately transported to the blood circulation via the subclavian vein. Thus, when the ALN is removed, normal lymph flow from the ILN is blocked and lymph congestion can occur. In order to investigate how internodal collecting lymphatic vessels change in response to axillary lymphadenectomy, we removed the ALN one min after i.d. injection of ICG to the base of the tail and imaged mice at different time points. As shown in Figs. 5(A) and 5(B), mice showed significantly higher fluorescent signal in the axillary region up to 4 hrs after axillary lymphadenectomy than the non-surgery group, due to ICG leakage in the axillary region. In addition, we observed dilated and tortuous fluorescent internodal collecting lymphatic vessels in mice after surgical removal of the ALN (inset in Fig. 5(A)) as compared to non-surgery mice. At 24 hrs post-surgery, there is no significant difference in the NIR fluorescent intensities between surgery and non-surgery groups (Fig. 5(B)). We also quantified lymphatic contractile function by selecting the same size of ROI at the same location in the internodal collecting lymphatic vessels in mice before and after axillary lymphadenectomy. Our quantification data showed a significantly reduced lymphatic contraction frequency for 5 mins at 10 min after axillary lymphadenectomy as compared to baseline (i.e., prior to surgery).

Next we tracked collecting lymphatics and examined if those vessels are dilated. Since, like ICG, EBD injection to the base of the tail did not delineate internodal collecting lymphatic vessels at 2 days post-surgery, EBD was injected directly into the ILNs, which were then pressed using a cotton swab. As shown in Fig. 6, enlarged EBD-filled collecting lymphatic vessels and abnormal branching (arrows) of lymphatic vessels, together with a dilated superficial epigastric vein, were observed in the left ipsilateral side as compared to contralateral right side. We also observed backflow in the left side of mice at Day 2 (Fig. 7). Our intravital imaging data was confirmed by H&E examination. The quantification of the vessel area demonstrated significantly increased vessel area of collecting lymphatic vessels on the surgical side as compared to contralateral control side at Day 2 (Fig. 6(E)). However, at 6 days post-surgery, no significant difference of the vessel area between left and right sides was observed (Fig. 6(F)).

#255572 Received 14 Dec 2015; revised 8 Feb 2016; accepted 26 Feb 2016; published 3 Mar 2016

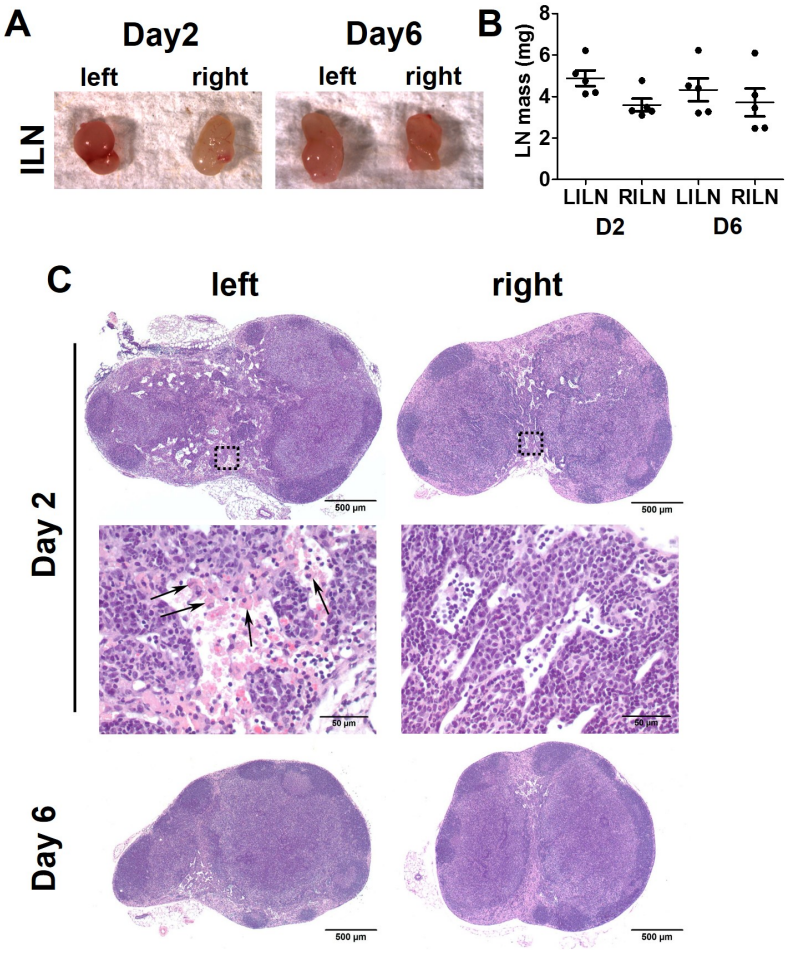

Fig. 8. A. Intravital images of dissected left and right ILNs 2 and 6 days after axillary lymphadenectomy. B. The quantification of weight of the ILNs (n = 5/group). C. H&E and zoomed in images of left and right ILNs at 2 and 6 days post-surgery. Arrow, phagocytes containing erythrocytes (erythrophagocytosis).

3.4. Lymph node analysis

Given that mice showed lymphatic congestion in the dilated internodal lymphatic vessels connecting from the ILN to the ALN, which had been removed 2 days before, we next sought to investigate how the upstream ILN changes in response to changes in lymph flow dynamics after surgical removal of the downstream ALN. As shown in Fig. 8(A), we observed that the ipsilateral ILNs, where lymph moves to the downstream axillary region via collecting lymphatic vessels, were in red and their weights were not significantly different from those in the contralateral ILN at day 2 (Fig. 8(B)). However, histologically, on Day 2, the ipsilateral upstream ILN were characterized by disorganized distended medullary sinuses (edema) which contain erythrocytes and erythrophagocytosis (arrows in Fig. 8(C)), whereas the contralateral RILN shows clean narrow medullary sinuses which do not contain erythrocytes but rather a normal population of circulating lymphoid cells. On Day 6, no significant lesions were observed on the ipsilateral and contralateral upstream ILNs.

#255572 Received 14 Dec 2015; revised 8 Feb 2016; accepted 26 Feb 2016; published 3 Mar 2016

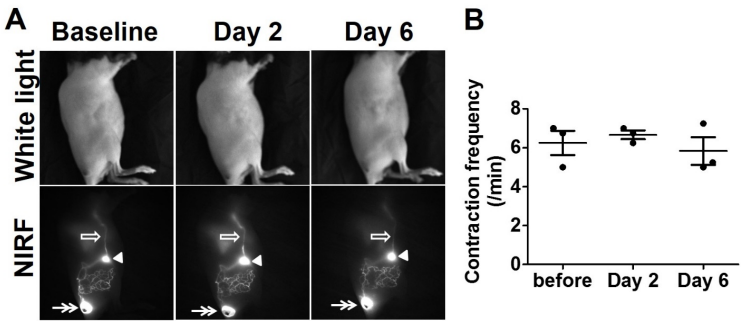

Fig. 9. (A) White light and NIR fluorescent images of right side of mice prior to and 2 and 6 days after surgical removal of the left ALN. Double arrow, ICG injection site. Arrow head, ILN. Open arrow, internodal collecting lymphatic vessels. Arrow head, ILN. Open arrow, internodal collecting lymphatic vessels. Double arrows, ICG injection site. (B) Quantification of lymphatic contractile function in the collecting lymphatic vessel in the contralateral right side of mice (n = 3) prior to and 2 and 6 days after left axillary lymphadenectomy.

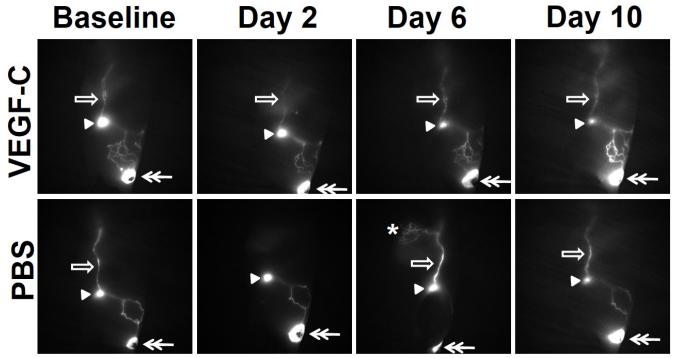

Fig. 10. NIR fluorescent images of VEGF-C (n = 11) or PBS (n = 5) treated mice prior to and 2, 6, and 10 days after surgical removal of the left ALN. Double arrow, ICG injection site. Arrow head, ILN. Open arrow, internodal collecting lymphatic vessels. Asterisk, aberrant lymphatic drainage to the contralateral ALN. Double arrows, ICG injection site.

3.5. No systemic effect on lymphatic drainage patterns or function after lymphadenectomy

In order to test if local lymphadenectomy resulted in systemic effect on lymphatic drainage patterns, we also imaged the right side of mice after left axillary lymphadenectomy. Our imaging data demonstrated the same lymphatic drainage patterns on the right side of mice before and 2 and 6 days after surgical removal of the left ALN as shown in Fig. 9(A). In addition, lymphatic contractile function did not change significantly over time (Fig. 9(B)), indicating that local lymphadenectomy does not affect systemic lymphatic function.

3.6. Effects of VEGF-C administration on lymphatic drainage after lymphadenectomy

It has been demonstrated that VEGF-C induces lymphangiogenesis, which can increase fluid drainage and thus prevent the buildup of fluid in the tissues under pathophysiological conditions. Although we observed naturally restored lymph transport as early as 9 days after lymphadenectomy, we asked whether VEGF-C administration can improve altered lymphatic drainage early after lymphadenectomy. As shown in Fig. 10, while all 5 mice treated with PBS as control showed no fluorescent collecting lymphatic vessels at day 2 post-surgery, 6 out of 11 mice treated with VEGF-C showed normal lymphatic drainage from the ILN to the axillary region via the collecting lymphatic vessels, indicating that VEGF-C administration helps maintain the connection to the drainage region.

#255572 Received 14 Dec 2015; revised 8 Feb 2016; accepted 26 Feb 2016; published 3 Mar 2016

4. Discussion

Interstitial fluid, macromolecules, and various other factors filtered out of blood capillaries are transported to initial lymphatics as lymph. Since LNs are arranged in chains or clusters, lymph is further fed to one or more LNs through conducting lymphatic vessels before returning to blood circulation via the subclavian vein. The afferent and efferent lymphatic vessels are separated by LNs. Thus, removal of a LN could have a significant impact on lymphatic transport. The BLN is the primary peripheral LN, which collects lymph from the front paw as well as the upper back. Lymph from the BLN drains to the secondary ALN, which also receives lymph from the ILN via internodal collecting lymphatic vessels. Therefore, surgical removal of the ALN can directly affect lymph flow in efferent brachial as well as inguinal collecting lymphatic vessels. In this study, we non-invasively imaged transient, but dramatic changes of lymphatic drainage patterns in efferent inguinal (i.e., internodal) collecting lymphatic vessels draining from the ILN to the axillary region after axillary lymphadenectomy.

When collecting lymphatic vessels are injured after trauma, such as lymphadenectomy, lymph starts to leak into the injured area. We observed significantly increased fluorescent intensities in the axillary area for up to 4 hrs (Fig. 5(B)); however, leaked ICG-laden lymph eventually cleared (Fig. 5(B)), although NIRF in the axilla was still detectable 24 hrs after surgery (Fig. 5(A)). In addition, since collecting lymphatic vessels at the wound area were obstructed and could not transport lymph downstream properly as evidenced by decreased lymphatic contractile function (Fig. 5(C)), the pressure in the collecting lymphatic vessels might increase gradually [19]. Thus, the conducting lymphatic vessels became dilated and tortuous (inset in Fig. 5(A)). Thus, at day 2 post surgery, we observed no NIR fluorescent internodal collecting lymphatic vessels connecting from the ILN and the axillary region. This is mainly due to continuously increased resistance to flow as a result of obstructed lymphatics in the axilla after surgery. Future study is needed to investigate what other factors also affect lymphatic vessel dilation. External compression on the upstream ILN enabled detection of a small segment of the internodal collecting lymphatic vessels draining from the ILN and the vessels became functional as demonstrated by active contractile function from NIRFI (Fig. 4(B)). However, alternate drainage through collateral lymphatic vessels was not always detected at day 2, even after compression. Previously, we observed rapid appearance of collateral lymphatic vessels draining to the ILN from the hind limb of mice 2 days after popliteal lymphadenectomy [9]. Development of collateral circulation may reduce or repair impaired lymph flow caused by surgical node removal. At day 2 post-surgery, FRFI following i.d. injection of Alexa680-BSA to the dorsal aspect of the front paw did not show abnormal lymphatic drainage on the operated limb of all mice. This is because lymphatic drainage to the BLN from the front paw was not directly disrupted in mice after surgical removal of the ALN. Likewise, we found similar patterns of afferent (i.e., pre-nodal) inguinal lymphatic vessels in mice after surgery as compared to those prior to surgery due to no disruption of normal lymph flow from the base of the tail to the ILN.

The lymphatic capillaries interconnect and join together to form collecting lymphatic vessels, which contain a series of lymphangions. Lymphangions are the functional contractile unit of lymphatic vessels and are bounded by intraluminal valves, which prevent backflow. Under physiological conditions, lymph enters lymphatic capillaries and flows forward due to a pressure gradient within collecting lymphatic vessels aided by one-way valves. Lymphatic valves are located at branch points in the collecting lymphatic vessels to prevent backflow of the lymph into the side branch [20]. Thus, normal mice prior to surgery did not show ICG-laden lymph flow to lymphatic vessels branching from the internodal collecting vessels. Previously, the internodal collecting lymphatic vessels draining from the ILN to the ALN have been utilized to (i) deliver a drug to the downstream ALN after internodal injection to the upstream ILN and (ii) study inter-LN metastasis between the ILN and the ALN [21, 22], due to easy identification of pre- and post-nodal lymphatic vessels. In addition, Karnezis *et al.* [23] showed VEGF-D overexpressing tumors resulted in collecting lymphatic vessel dilation

#255572 Received 14 Dec 2015; revised 8 Feb 2016; accepted 26 Feb 2016; published 3 Mar 2016

and thus an increase in cancer metastasis to the ALN. In general, the collecting lymphatic vessels draining from the ILN to the ALN showed zero to three bifurcations, which depend upon mouse strain, even mouse to mouse in the same strain [11, 22]. However, under pathological conditions, lymph may not flow down a pressure gradient. Previously, we observed branching of collecting lymphatic vessels, resulting in lateral lymph flow and backflow in mice with lymphatic disorders [11, 14]. In current studies, at 6 days after axillary lymphadenectomy, extensive lymphatic network draining from the left ILN to the ipsilateral BLN and to the contralateral ALN through branched lymphatic vessels and, in some mice, to the contralateral cervical LN across the midline of the body was visualized. Abnormal lymphatic drainage patterns started to disappear beginning 9 days after surgery.

Previously Hall *et al.* [24] demonstrated changes of lymphatic vessel drainage after flank incision on the animal's left side, which interrupted normal lymph flow in the internodal collecting lymphatic vessels draining from the ILN to the ALN. Similar to our current findings, in their mouse full-dermis thickness wound model, fluorescent lymphatic vessels were not visualized during early stage (i.e., day 2 to 3 post-incision) of wound healing, but numerous fluorescent lymphatic vessels on the wounded side were detected from 7 – 8 days up to 2-3 weeks after wounding. They also showed minimal effects of a single injection of vascular endothelial growth factor (VEGF)-C at day 1 post-incision on wound healing and regression of abnormal lymphatic drainage patterns at day 7-8, although cytokines/chemokines responded to some extent to VEGF-C administration. Previous studies have demonstrated that VEGF-C gene transfer or application of recombinant VEGF-C protein induces lymphangiogenesis, thereby improving edema resolution [25–27]. A recent study also demonstrated that a single injection of recombinant VEGF-C increased sprouting and proliferation of Schlemm's canal endothelial cells, resulting in a decrease in intraocular pressure in adult mice and thus improvement of drainage through Schlemm's canal [28]. In addition, peritumoral administration of VEGF-C 7 days after tumor cell injection in mice lowered tumor-interstitial fluid pressure by enhancing lymphatic drainage of the tumor interstitium [29]. Our study using NIRFI also demonstrated that VEGF-C application to the surgical region in mice after lymphadenectomy accelerates resolution of experimentally induced alteration in lymphatic drainage by reducing increased interstitial pressure in mice after axillary lymphadenectomy (Fig. 10), although we showed natural restoration of altered lymph transport as early as 9 days post-surgery (Figs. 2 and 3).

A recent study by Sweet *et al*. [30] demonstrated the functional role of lymph flow in valve formation and collecting lymphatic vessel maturation and development. Therefore, it is possible that long-term interruption of lymph flow might cause collecting lymphatic vessel dysfunction and thus contribute to chronic lymphatic disorders. In addition to collecting lymphatic vessels, lymph flow can affect functional integrity of LNs. Mebius *et al.* [31] showed that experimental occlusion of the afferent vessels to mouse popliteal LNs leads to changes in morphology and function of high endothelial venules (HEV). In addition, after blockage of afferent popliteal lymphatic vessels, the popliteal LN was reduced in size and all lymphoid structures, such as germinal centers and lymph follicles, were also decreased in size and number [32, 33], which is mainly due to reduced afferent (incoming) lymph of antigens and other factors. In contrast, blockage of efferent popliteal lymphatic vessels caused an increase in size and large lymph space as represented by dilated lymphatic sinuses containing scanty numbers of lymphocytes and macrophages [33]. It has also been shown that lymph stasis after ligation of efferent lymphatic vessels produced swelling of the PLN (i.e., edematous LN) and medullary sinuses and possibly fibrosis [33, 34]. Although lymphatic obstruction by surgical removal of the downstream ALN is not as significant as complete ligation of efferent lymphatic vessels, we also observed transient morphological changes in the ipsilateral upstream ILN, where expanded disorganized medullary sinuses which contain erythrocytes and phagocytes containing erythrocytes. Long-term occlusion of the efferent lymphatic vessels resulted in thickening of the LN capsule and sclerosis of the medullary sinuses [34]. Taken together, LN homeostasis is maintained by not only functioning afferent, but also efferent lymphatic vessels.

#255572 Received 14 Dec 2015; revised 8 Feb 2016; accepted 26 Feb 2016; published 3 Mar 2016

In this study, we used dual-wavelength fluorescence imaging with injection of Alexa-680-BSA (excitation: 660nm and emission: 710nm) and ICG (excitation: 785nm and emission: 830nm) to the paw and to the base of the tail, respectively, to image lymphatic vessels in different regions. Whole-body FRFI showed diet-induced fluorescence in the abdomen of mice as shown in Fig. 2. It has been reported that chlorophyll from the alfalfa in commonly used laboratory murine diets fluoresces between 650 to 750nm [17]. Therefore, when mice are excited by 660nm excitation light, strong background fluorescence resulting from ingested food along the gastrointestinal (GI) tract in the abdominal region is detected, which may provide a significant limitation for in vivo fluorescence imaging, especially using red excitable fluorophores. However, diet-induced fluorescence can be eliminated using chlorophyll free food or multiplexing imaging. Unlike FRFI, NIRF imaging can be advantageous for non-invasive tissue imaging due to low tissue absorption and scattering and lack of background fluorescence.

In summary, we successfully demonstrate transient, but dramatic changes of different lymphatic drainage patterns in the internodal collecting lymphatic vessels draining from the ILN to the axillary region after surgical removal of a single ALN. Based upon our finding, NIRFI can be used as a means to non-invasively and longitudinally monitor lymphatic responses to cancer treatments, such as surgery and radiation therapy, and potentially assess new strategies to treat and prevent lymphatic disorders.

Acknowledgments

The authors would like to thank Holly Robinson and Karen Gore for technical assistance with the mice used in these experiments and Drs. Melissa B. Aldrich, Cynthia Davies-Venn, and Eva M. Sevick-Muraca for scientific review of manuscript. This work was supported in part by the National Institutes of Health R21 CA159193 (SK).

#255572 Received 14 Dec 2015; revised 8 Feb 2016; accepted 26 Feb 2016; published 3 Mar 2016